Research Square

Preprints are preliminary reports that have not undergone peer review.
They should not be considered conclusive, used to inform clinical practice,
or referenced by the media as validated information.

Group-theoretic and equivalence-symmetry analysis of a susceptible–infected–AIDS HIV model

Samuel Okon Essang

sammykmf@gmail.com

Landmark University https://orcid.org/0009-0000-9165-5819

Research Article

Keywords: Lie point symmetry, Equivalence transformation, HIV/AIDS model, Solvable Lie algebra, Basic reproduction number

Posted Date: August 3rd, 2026

DOI: https://doi.org/10.21203/rs.3.rs-10541318/v1

License: This work is licensed under a Creative Commons Attribution 4.0 International License.
Read Full License

Additional Declarations: The authors declare no competing interests.

Group-theoretic and equivalence-symmetry analysis of a susceptible–infected–AIDS HIV model

Samuel O. Essang[1] B. I. N.-I. Iserom[2] Timothy Ashibel Anake[3]

[1]Mathematics Programme, Department of Physical Science, Landmark University, Omu-Aran, Kwara State, Nigeria
[2]Group Theory Unit, Department of Pure and Industrial Chemistry, University of Calabar, Calabar, Cross River State, Nigeria
[3]Department of Mathematics, Covenant University, Ota, Ogun State, Nigeria

Corresponding author: Samuel O. Essang, essang.samuel@lmu.edu.ng
ORCID (S. O. Essang): 0009-0000-9165-5819

Abstract

In group theory, symmetry belongs to a single model or to a whole family of models, and most time, conflating the two invalidates any reduction built on it. This paper pin points the difference clearly for a three-compartment susceptible–infected–AIDS model of HIV transmission as the case may be. The nonnegative octant is revealed to be forward invariant, every solution is bounded, with disease-free and endemic equilibria are separated by the basic reproduction number. Putting to test Lie point symmetry directly through the first prolongation, we establish that time translation is the only elementary symmetry admitted when the parameters are held fixed, and that the population scalings commonly assumed for compartmental models violate the determining equations outright. Those scalings are rehabilitated only as *equivalence* transformations, once the recruitment and transmission parameters are rescaled in step with the populations. Together with time dilation this yields a solvable three-parameter equivalence group whose invariants collapse five parameters to three and return a compact dimensionless model. An independent numerical experiment confirms the equivalence group to eleven significant figures, and the reduced flow reproduces the transcritical threshold, the endemic equilibrium, and the parameter sensitivities of the full system exactly. The analysis absolutely gives a reproducible template for distinguishing genuine symmetries from model-family equivalences in richer HIV models, including those with treatment, age structure, then spatial spread.

Keywords Lie point symmetry · Equivalence transformation · HIV/AIDS model · Solvable Lie algebra · Basic reproduction number

Mathematics Subject Classification 92D30 · 34C14 · 22E70 · 34A34

Acknowledgements The authors thank their respective institutions for the research environment in which this work was carried out.

1 Introduction

In most cases, mathematical models of HIV transmission are used to locate epidemic thresholds, to compare interventions, and to quantify how treatment, prevention, demographic structure, and uncertainty shape the course of the disease. The recent literature is broad. Fractional and fractal–fractional operators encode memory and nonlocal progression (Silva and Torres 2019; Naik et al 2020a;b; Khan et al 2025); age structure and optimal control target the interventions that matter most in practice (Teklu et al 2025); drug resistance and vertical transmission add realism at the cost of extra compartments (Peter et al 2025); and country-specific studies calibrate transmission and control to national data in Indonesia and China (Abidemi et al 2025; Xue et al 2023; Su et al 2026). Usually the SICA family of Silva and Torres and its stochastic and control-theoretic descendants remain a standard deterministic backbone for this activity (Silva and Torres 2017; 2018; Djordjevic et al 2018; Silva and Torres 2020; Attaullah et al 2023). What actually unites these efforts is a parameter-first stance: one fixes numerical values and then simulates, calibrates, or optimizes as the case may be.

Actually, we know that Lie symmetry analysis approaches the same equations from the opposite direction. Rather than beginning with parameter values, it asks which continuous transformations preserve a differential equation, and it extracts reductions, invariant variables, exact solutions, and equivalence relations from the answer (Hydon 2000; Olver 1993; Bluman et al 2010; Ibragimov 1994). The method has become active in epidemiology: Indeed, Lie analyses of reaction–diffusion–advection SIS systems yield closed-form travelling waves (Naz et al 2025; Naz and Torrisi 2024), and age-structured or cross-diffusive pandemic models admit symmetry reductions that would be invisible to a purely numerical treatment (Cherniha and Davydovych 2025; Cherniha et al 2024; Cherniha and Davydovych 2022) accordingly.

A single distinction governs whether such an analysis is sound. A *point symmetry* maps solutions of one fixed model to other solutions of the same model; an *equivalence transformation* maps one model of a family to another model of the same family, typically by moving the parameters as well as the states. The two objects look alike on paper which is both are generated by vector fields, both produce invariants and yet they answer different questions. A quantity that is invariant under an equivalence group is constant across the family, not along a single trajectory, and treating it as a conserved quantity of the dynamics is simply an error. The confusion is easy to commit because tangency to the level set of a candidate first integral is visually suggestive; it is, however, neither necessary nor sufficient for the prolonged invariance criterion to hold if we consider it closely.

This paper carries out the distinction in full for a basic susceptible–infected–AIDS model. The objectives are fourfold: (i) to establish the dynamical foundation for which invariance of the state space, boundedness, and the threshold structure controlled by the basic reproduction number (Diekmann et al 1990; van den Driessche and Watmough 2002); (ii) to test the elementary Lie point symmetries directly against the determining equations, confirming time translation and rejecting the naive scal-

ing; (iii) to identify the valid equivalence group on the joint state–parameter space and to describe its Lie algebra; and (iv) to derive the scaling invariants, the reduced dimensionless model, and its dynamics, with every analytic claim checked numerically. Actually, no nonconstant first integral is assumed anywhere. It is good to note that the contribution is not a new epidemiological mechanism but a corrected and reusable symmetry template: it shows precisely how far continuous symmetry reaches for this class of models, and it supplies a reduction that any downstream calibration or control study can as well adopt without re-deriving.

Thought it all, the paper is organized as this way. Section 2 formulates the model and proves positivity, boundedness, and the threshold. Section 3 sets up the prolongation formalism and tests the elementary generators. Section 4 constructs the equivalence group and its algebra and verifies it numerically, then section 5 derives the scaling invariants and the reduced model. Section 6 studies the reduced dynamics, the transcritical bifurcation, and the sensitivity of the threshold. Section 7 now treats symmetry breaking under time-dependent interventions. Sections 8 and 9 discuss the findings and gives the conclusion.

2 Model formulation and basic properties

2.1 The susceptible–infected–AIDS model

Let $S(t)$ denote the susceptible population, $I(t)$ the HIV-infected individuals who have not progressed to AIDS, and $A(t)$ the individuals in the AIDS stage. The model is

$$\dot{S} = \Sigma - \gamma SI - \alpha S, \tag{1}$$

$$\dot{I} = \gamma SI - (\alpha + \omega)\, I, \tag{2}$$

$$\dot{A} = \omega I - (\alpha + \delta)\, A. \tag{3}$$

All parameters are nonnegative, with $\Sigma > 0$ and $\alpha > 0$. Only the I compartment transmits infection in this baseline; the AIDS class is taken to be noninfectious, a deliberate simplification examined in Section 8. Table 1 lists the state variables and parameters.

2.2 Positivity, boundedness, and an absorbing region

Proposition 1 (Positivity and boundedness)**.** *For every nonnegative initial condition* (S_0, I_0, A_0)*, system* (1)–(3) *has a unique nonnegative solution on its maximal interval of existence. Every solution is bounded, and the region*

$$\Omega = \left\{ (S, I, A) \in \mathbb{R}^3_{\geq 0} :\ S + I + A \leq \tfrac{\Sigma}{\alpha} \right\} \tag{4}$$

is positively invariant and absorbing.

Table 1 State variables and parameters of model (1)–(3).

Symbol	Interpretation	Units
S	susceptible population	individuals
I	HIV-infected population without AIDS	individuals
A	population in the AIDS stage	individuals
Σ	recruitment rate into the susceptible class	individuals time^{-1}
γ	effective HIV transmission coefficient	individuals^{-1}time^{-1}
α	natural mortality rate	time^{-1}
ω	progression rate from HIV infection to AIDS	time^{-1}
δ	additional AIDS-induced mortality rate	time^{-1}

Proof. The vector field of (1)–(3) is polynomial, hence locally Lipschitz, so a unique local solution exists. On the coordinate faces of the nonnegative octant the field points inward or is tangent: when $S = 0$ one has $\dot{S} = \Sigma > 0$; when $I = 0$ one has $\dot{I} = 0$; and when $A = 0$ one has $\dot{A} = \omega I \geq 0$. Consequently the nonnegative octant is forward invariant. Writing $N = S + I + A$ and summing (1)–(3),

$$\dot{N} = \Sigma - \alpha N - \delta A \leq \Sigma - \alpha N. \tag{5}$$

The differential inequality (5) together with the comparison theorem gives

$$N(t) \leq N(0)\, e^{-\alpha t} + \frac{\Sigma}{\alpha}\big(1 - e^{-\alpha t}\big), \tag{6}$$

so $\limsup_{t\to\infty} N(t) \leq \Sigma/\alpha$. Boundedness follows, and (6) shows every trajectory enters and remains in Ω; the solution therefore extends to all $t \geq 0$. □

2.3 Equilibria and the basic reproduction number

Proposition 2 (Threshold and equilibria)**.** *The disease-free equilibrium of* (1)–(3) *is*

$$E_0 = \Big(\tfrac{\Sigma}{\alpha},\, 0,\, 0\Big), \tag{7}$$

and the basic reproduction number is

$$\mathcal{R}_0 = \frac{\gamma\Sigma}{\alpha(\alpha + \omega)}. \tag{8}$$

E_0 is locally asymptotically stable when $\mathcal{R}_0 < 1$ and unstable when $\mathcal{R}_0 > 1$. For $\mathcal{R}_0 > 1$ a unique endemic equilibrium $E_e = (S_e, I_e, A_e)$ exists, with

$$S_e = \frac{\alpha + \omega}{\gamma}, \qquad I_e = \frac{\alpha(\mathcal{R}_0 - 1)}{\gamma}, \qquad A_e = \frac{\omega\alpha(\mathcal{R}_0 - 1)}{\gamma(\alpha + \delta)}. \tag{9}$$

Proof. Setting the right-hand sides of (1)–(3) to zero with $I = 0$ gives E_0. To obtain $\mathcal{R}_0$ we use the

next-generation construction (Diekmann et al 1990; van den Driessche and Watmough 2002). The single infected compartment is I; the new-infection and transition terms are

$$\mathcal{F} = \gamma S I, \qquad \mathcal{V} = (\alpha + \omega) I, \tag{10}$$

so that at E_0, where $S = \Sigma/\alpha$, the next-generation quantity is the scalar

$$\mathcal{R}_0 = \left. \frac{\partial \mathcal{F}/\partial I}{\partial \mathcal{V}/\partial I} \right|_{E_0} = \frac{\gamma \Sigma/\alpha}{\alpha + \omega} = \frac{\gamma \Sigma}{\alpha(\alpha + \omega)}. \tag{11}$$

The Jacobian of (1)–(3) at E_0 is lower-block-triangular,

$$J(E_0) = \begin{pmatrix} -\alpha & -\gamma\Sigma/\alpha & 0 \\ 0 & \gamma\Sigma/\alpha - (\alpha+\omega) & 0 \\ 0 & \omega & -(\alpha+\delta) \end{pmatrix}, \tag{12}$$

with eigenvalues $-\alpha$, $-(\alpha+\delta)$, and $\gamma\Sigma/\alpha - (\alpha+\omega) = (\alpha+\omega)(\mathcal{R}_0 - 1)$. The last changes sign at $\mathcal{R}_0 = 1$, which gives the stated local threshold. Solving the steady-state equations with $I > 0$ yields (9): from (2), $\gamma S_e = \alpha + \omega$; substituting into (1) gives I_e; and (3) gives A_e. Both I_e and A_e are positive precisely when $\mathcal{R}_0 > 1$. □

3 Lie point symmetry test

3.1 Generators, prolongation, and determining equations

Write the system (1)–(3) as a first-order autonomous field $\dot{x}_i = F_i(x)$ with $x = (S, I, A)$. A point-symmetry generator has the form

$$Q = \tau(t, x)\, \partial_t + \sum_{i=1}^{3} \eta_i(t, x)\, \partial_{x_i}. \tag{13}$$

Its first prolongation, needed because the invariance condition acts on the first derivatives, is

$$\mathrm{pr}^{(1)} Q = Q + \sum_{i=1}^{3} \eta_i^{(1)}\, \partial_{\dot{x}_i}, \qquad \eta_i^{(1)} = D_t \eta_i - \dot{x}_i\, D_t \tau, \tag{14}$$

where D_t is the total time derivative. The generator Q is admitted if and only if

$$\mathrm{pr}^{(1)} Q\, (\dot{x}_i - F_i)\big|_{\dot{x} = F} = 0, \qquad i = 1, 2, 3. \tag{15}$$

Equation (15) supplies the determining equations, which must be checked term by term; no shortcut through candidate invariants replaces them.

Remark 1. A first integral $J(x)$ satisfies $F(J) = \nabla J \cdot F = 0$, i.e. its level sets are tangent to the flow. A vector field tangent to those level sets need not satisfy (15): tangency is a statement about J, whereas (15) is a statement about the prolonged action of Q on the equations. The existence of a first integral therefore does not by itself produce an additional point symmetry, and the determining equations remain the only admissible test.

3.2 Time-translation symmetry

Proposition 3 (Time translation)**.** *For fixed parameters, system* (1)–(3) *admits the one-parameter group*

$$\bar{t} = t + \varepsilon, \qquad (\bar{S}, \bar{I}, \bar{A}) = (S, I, A), \tag{16}$$

with infinitesimal generator

$$X_0 = \partial_t. \tag{17}$$

Proof. The field F in (1)–(3) does not depend on t. For $Q = \partial_t$ one has $\tau = 1$, $\eta_i = 0$, hence $\eta_i^{(1)} = 0$ by (14), and (15) reduces to $-\partial_t F_i = 0$, which holds because the system is autonomous. Equivalently, if $(S, I, A)(t)$ solves the system then so does $(S, I, A)(t + \varepsilon)$. □

3.3 Failure of the elementary state scalings

Two population scalings suggest themselves as candidate symmetries: the uniform scaling Q_N of all three states, and the scaling Q_{IA} of the two infected classes,

$$Q_N = S\,\partial_S + I\,\partial_I + A\,\partial_A, \qquad Q_{IA} = I\,\partial_I + A\,\partial_A. \tag{18}$$

Both have $\tau = 0$, so $\eta_i^{(1)} = D_t \eta_i$, and (15) becomes $\mathrm{pr}^{(1)} Q(\dot{x}_i - F_i) = D_t \eta_i - Q(F_i) = 0$ on solutions. Denote by $\mathcal{R}(Q) = (\mathcal{R}_1, \mathcal{R}_2, \mathcal{R}_3)$ the resulting residual vector. A direct computation gives, for Q_N,

$$\mathcal{R}(Q_N) = \big(\Sigma + \gamma SI,\ -\gamma SI,\ 0\big), \tag{19}$$

and, for Q_{IA},

$$\mathcal{R}(Q_{IA}) = \big(\gamma SI,\ 0,\ 0\big). \tag{20}$$

Neither residual vanishes for generic positive Σ and γ: the constant recruitment term Σ and the bilinear incidence γSI break the scale invariance. Hence *neither Q_N nor Q_{IA}* is a point symmetry of the fixed-parameter model. Table 2 collects the outcome of the elementary tests.

Table 2 Outcome of the elementary Lie point symmetry tests for fixed parameters. Only time translation is admitted; the population scalings leave non-vanishing residuals and are rejected.

Generator	Action	Prolonged residual $\mathcal{R}(Q)$	Admitted?
$X_0 = \partial_t$	time translation	$(0, 0, 0)$	Yes
$Q_N = S\partial_S + I\partial_I + A\partial_A$	uniform state scaling	$(\Sigma + \gamma SI,\, -\gamma SI,\, 0)$	No
$Q_{IA} = I\partial_I + A\partial_A$	infected-class scaling	$(\gamma SI,\, 0,\, 0)$	No

4 Equivalence group on the extended state–parameter space

4.1 The three-parameter equivalence group

The scalings fail as point symmetries because the parameters are held fixed. If instead the parameters are allowed to move with the states, the same scalings map one model of the family (1)–(3) to another and become *equivalence* transformations.

Proposition 4 (Three-parameter equivalence group)**.** *The family* (1)–(3) *is closed under*

$$\bar{t} = e^{\varepsilon_1} t + \varepsilon_0, \qquad (\bar{S}, \bar{I}, \bar{A}) = e^{\varepsilon_2}(S, I, A), \tag{21}$$

provided the parameters transform as

$$\bar{\Sigma} = e^{\varepsilon_2 - \varepsilon_1}\Sigma, \quad \bar{\gamma} = e^{-(\varepsilon_1 + \varepsilon_2)}\gamma, \quad \bar{\alpha} = e^{-\varepsilon_1}\alpha, \quad \bar{\omega} = e^{-\varepsilon_1}\omega, \quad \bar{\delta} = e^{-\varepsilon_1}\delta. \tag{22}$$

Proof. From (21), $\mathrm{d}\bar{t} = e^{\varepsilon_1}\mathrm{d}t$ and $\mathrm{d}\bar{S} = e^{\varepsilon_2}\mathrm{d}S$, so $\mathrm{d}\bar{S}/\mathrm{d}\bar{t} = e^{\varepsilon_2 - \varepsilon_1}\dot{S}$, with the analogous identities for $\bar{I}$ and $\bar{A}$. Substituting (1) and expressing S, I through the barred states $S = e^{-\varepsilon_2}\bar{S}$, $I = e^{-\varepsilon_2}\bar{I}$,

$$\frac{\mathrm{d}\bar{S}}{\mathrm{d}\bar{t}} = e^{\varepsilon_2 - \varepsilon_1}\big(\Sigma - \gamma SI - \alpha S\big) = e^{\varepsilon_2 - \varepsilon_1}\Sigma - \gamma e^{-\varepsilon_1 - \varepsilon_2}\bar{S}\bar{I} - \alpha e^{-\varepsilon_1}\bar{S} = \bar{\Sigma} - \bar{\gamma}\,\bar{S}\bar{I} - \bar{\alpha}\,\bar{S}. \tag{23}$$

The same substitution turns (2) and (3) into $\mathrm{d}\bar{I}/\mathrm{d}\bar{t} = \bar{\gamma}\bar{S}\bar{I} - (\bar{\alpha} + \bar{\omega})\bar{I}$ and $\mathrm{d}\bar{A}/\mathrm{d}\bar{t} = \bar{\omega}\bar{I} - (\bar{\alpha} + \bar{\delta})\bar{A}$. The barred system has the same form as the original, which proves closure. □

4.2 Infinitesimal generators and the Lie algebra

Let Y_r and Y_x denote the parameter and state Euler fields

$$Y_r = -\big(\alpha\,\partial_\alpha + \omega\,\partial_\omega + \delta\,\partial_\delta\big), \qquad Y_x = S\,\partial_S + I\,\partial_I + A\,\partial_A. \tag{24}$$

Differentiating (21)–(22) at the identity with respect to $\varepsilon_0, \varepsilon_1, \varepsilon_2$ gives the generators of the equivalence group on the extended space $(t, S, I, A, \Sigma, \gamma, \alpha, \omega, \delta)$:

$$X_0 = \partial_t, \tag{25}$$

$$X_1 = t\,\partial_t - \Sigma\,\partial_\Sigma - \gamma\,\partial_\gamma + Y_r, \tag{26}$$

$$X_2 = Y_x + \Sigma\,\partial_\Sigma - \gamma\,\partial_\gamma. \tag{27}$$

Here X_0 is time translation, X_1 is the time dilation that also contracts all rate parameters, and X_2 is the population dilation that rescales Σ and γ oppositely. Their commutators are

$$[X_0, X_1] = X_0, \qquad [X_0, X_2] = 0, \qquad [X_1, X_2] = 0. \tag{28}$$

So, the only non-vanishing bracket is $[X_0, X_1] = X_0$; the two dilations commute. The algebra is therefore solvable and nonabelian, with the derived algebra $\mathrm{span}\{X_0\}$ one-dimensional. This structure is exactly what a clean scaling reduction requires: the commuting pair $\{X_1, X_2\}$ supplies two independent dilations whose joint invariants define the dimensionless variables of Section 5.

4.3 Numerical verification of the equivalence transformation

However, Proposition 4 is an identity, but an independent numerical check guards against algebraic slips and demonstrates the practical meaning of the group. We integrate the base model with $(\Sigma, \gamma, \alpha, \omega, \delta) = (2.0, 0.9, 0.5, 0.3, 0.2)$ and initial data $(S_0, I_0, A_0) = (3.0, 0.6, 0.2)$, and integrate a transformed model whose parameters follow (22) for the group element $(\varepsilon_0, \varepsilon_1, \varepsilon_2) = (0, \ln 1.7, \ln 0.6)$, started from the transformed initial data $e^{\varepsilon_2}(S_0, I_0, A_0)$. Mapping both solutions through the scaling invariants $\tau = \alpha t$ and $s = \alpha S/\Sigma$ (defined in Section 5) should collapse them onto a single reduced orbit. Figure 1 shows exactly this: the reduced trajectories of the two distinct dimensional models coincide, with maximum discrepancy 3.9×10^{-11}, at the level of the integrator tolerance. The experiment confirms that the transformation relates *different members of the family*, not different solutions of one model—the operational content of the point-vs. equivalence distinction.

5 Scaling invariants and dimensionless reduction

5.1 Invariants and the reduced model

Well, after fixing the time origin with the X_0 translation, the joint invariants of the commuting dilations X_1 and X_2 define the dimensionless time, states, and parameters

$$\tau = \alpha t, \quad s = \frac{\alpha S}{\Sigma}, \quad i = \frac{\alpha I}{\Sigma}, \quad a = \frac{\alpha A}{\Sigma}, \qquad \beta = \frac{\gamma \Sigma}{\alpha^2}, \quad q = \frac{\omega}{\alpha}, \quad d = \frac{\delta}{\alpha}. \tag{29}$$

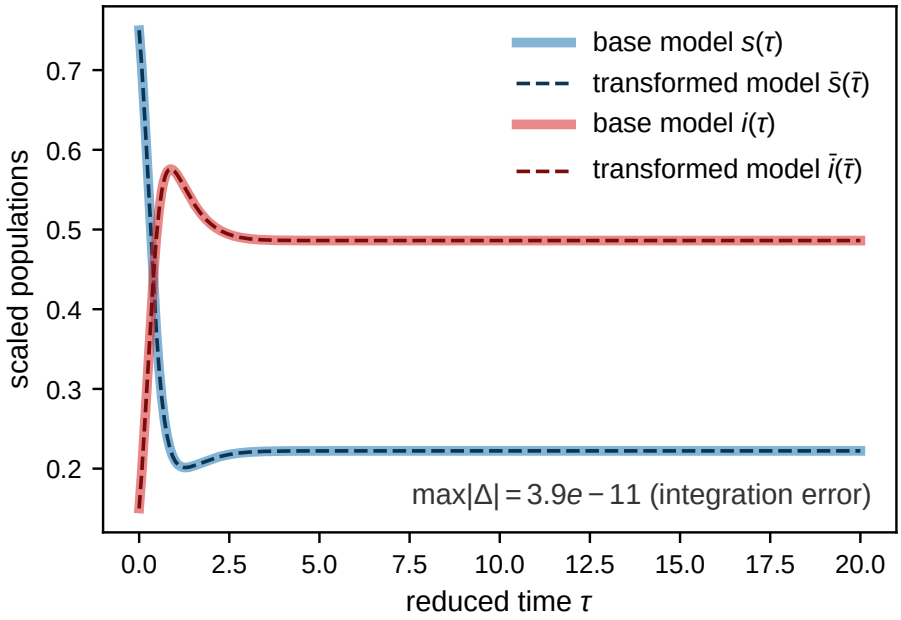

Fig. 1 Numerical verification of the equivalence group of Proposition 4. A base dimensional model (thick, translucent) and a transformed model obtained from (22) (dashed) are integrated independently and mapped through the scaling invariants $\tau = \alpha t$, $s = \alpha S/\Sigma$, $i = \alpha I/\Sigma$. The two reduced orbits coincide to 3.9×10^{-11}, the integration-error floor

Table 3 Dimensionless variables and parameters, defined as joint invariants of the commuting dilations X_1 and X_2.

Dimensionless quantity	Definition	Meaning
τ	αt	time in units of the demographic scale $1/\alpha$
s, i, a	$\alpha S/\Sigma,\ \alpha I/\Sigma,\ \alpha A/\Sigma$	populations in units of Σ/α
β	$\gamma\Sigma/\alpha^2$	transmission strength on the demographic scale
q	ω/α	progression relative to natural mortality
d	δ/α	excess AIDS mortality relative to natural mortality

Each quantity in (29) is annihilated by both X_1 and X_2, so it is constant along the equivalence orbits. Substituting (29) into (1)–(3) and using $\dot{}\mathrm{d}t = \alpha\,\dot{}\mathrm{d}\tau$ gives the reduced system

$$\frac{\mathrm{d}s}{\mathrm{d}\tau} = 1 - s - \beta s i, \tag{30}$$

$$\frac{\mathrm{d}i}{\mathrm{d}\tau} = \beta s i - (1+q)\, i, \tag{31}$$

$$\frac{\mathrm{d}a}{\mathrm{d}\tau} = q\, i - (1+d)\, a. \tag{32}$$

Table 3 records the dimensionless variables and parameters and their construction.

5.2 Reduced threshold and equilibria

In the reduced variables the basic reproduction number takes the compact form

$$\mathcal{R}_0 = \frac{\beta}{1+q}, \tag{33}$$

which agrees with (8) under (29). The reduced disease-free and endemic equilibria are

$$\widetilde{E}_0 = (1, 0, 0), \qquad \widetilde{E}_e = (s_e, i_e, a_e), \tag{34}$$

with

$$s_e = \frac{1}{\mathcal{R}_0}, \qquad i_e = \frac{1 - \mathcal{R}_0^{-1}}{1+q}, \qquad a_e = \frac{q\,(1 - \mathcal{R}_0^{-1})}{(1+q)(1+d)}. \tag{35}$$

Five dimensional parameters $(\Sigma, \gamma, \alpha, \omega, \delta)$ collapse to three independent combinations (β, q, d), and the qualitative phase portrait is preserved up to the rescaling of time and population units.

5.3 The invariant map

Let $z = (t, S, I, A, \Sigma, \gamma, \alpha, \omega, \delta)$. The dilation subgroup acts through the invariant map

$$\Pi(z) = (\pi_1, \pi_2, \pi_3, \pi_4, \pi_5, \pi_6, \pi_7), \tag{36}$$

with

$$(\pi_1, \pi_2, \pi_3, \pi_4) = \Big(\alpha t,\ \frac{\alpha S}{\Sigma},\ \frac{\alpha I}{\Sigma},\ \frac{\alpha A}{\Sigma}\Big), \qquad (\pi_5, \pi_6, \pi_7) = \Big(\frac{\gamma\Sigma}{\alpha^2},\ \frac{\omega}{\alpha},\ \frac{\delta}{\alpha}\Big). \tag{37}$$

Two models share an image under Π precisely when they lie on the same orbit of the dilation subgroup of Proposition 4; the seven entries of Π are a complete set of dilation invariants.

5.4 Analytic invariants and threshold geometry

Figures 2–4 display the exact analytic content of the reduction, with no empirical input. The threshold relation (33) partitions the (q, β) plane along the line $\beta = 1 + q$ (Figure 2); the same relation, drawn as a surface over the reduced parameter plane, is monotone increasing in β and decreasing in q (Figure 3). The scaling invariants $U_1 = I/A$ and $U_2 = S/(I + A)$ foliate their respective planes into straight rays (Figure 4); each ray is a level set carried into itself by the population dilation X_2.

6 Dynamics of the reduced model

The reduction is only useful if the reduced flow reproduces the epidemiology of the full model. We verify this by direct integration of (30)–(32), using a high-accuracy adaptive Runge–Kutta scheme

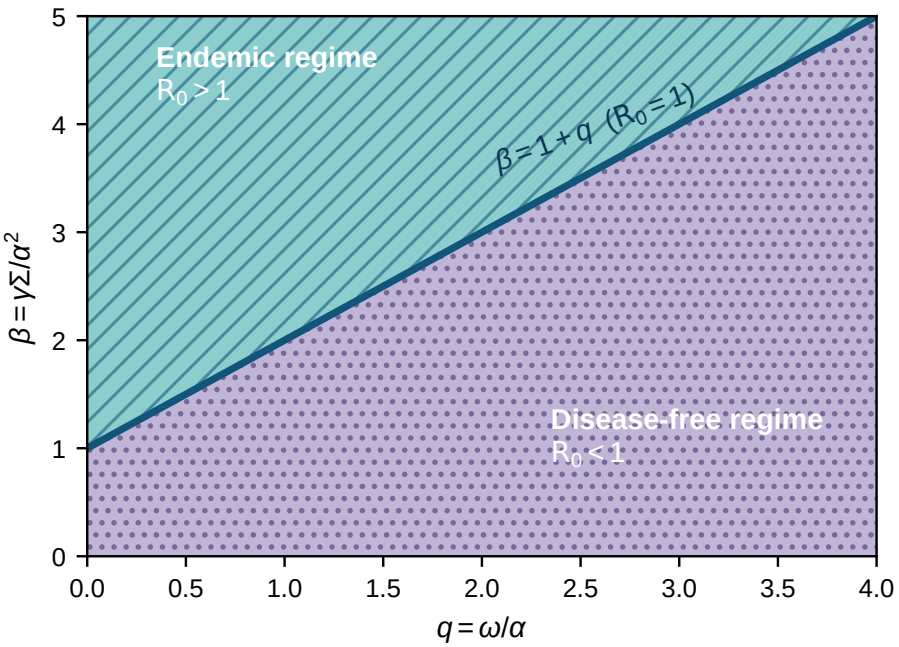

Fig. 2 Threshold partition of the (q, β) plane defined by $\mathcal{R}_0 = \beta/(1+q)$. The line $\beta = 1 + q$ separates the disease-free regime ($\mathcal{R}_0 < 1$) from the endemic regime ($\mathcal{R}_0 > 1$)

Table 4 Reduced parameter sets used in the numerical experiments of Section 6. Values are chosen to place the system on either side of the threshold; they are illustrative, not calibrated to data.

Regime	β	q	d	$\mathcal{R}_0 = \beta/(1+q)$
Disease-free (Fig. 5a)	0.8	0.6	0.5	0.50
Endemic (Figs. 5b,6)	4.0	0.6	0.5	2.50

with relative tolerance 10^{-9}; the parameter sets are listed in Table 4.

6.1 Trajectories and phase portrait

Clearly, Figure 5 shows the reduced states against τ. Below threshold the infected and AIDS classes decay to zero and the susceptible fraction relaxes to $s = 1$, i.e. to $\widetilde{E}_0$. Above threshold the trajectory settles at the endemic values (35), drawn as dotted lines; for the endemic set these are $(s_e, i_e, a_e) = (0.400, 0.375, 0.150)$, which the simulation reproduces. Figure 6 plots the (s, i) phase plane for the endemic set which shows that trajectories from a range of initial conditions spiral or bend into the endemic equilibrium (star), while the disease-free equilibrium (square) is a saddle emphatically. The reduced flow is thus globally organized by the same threshold that governs (1)–(3).

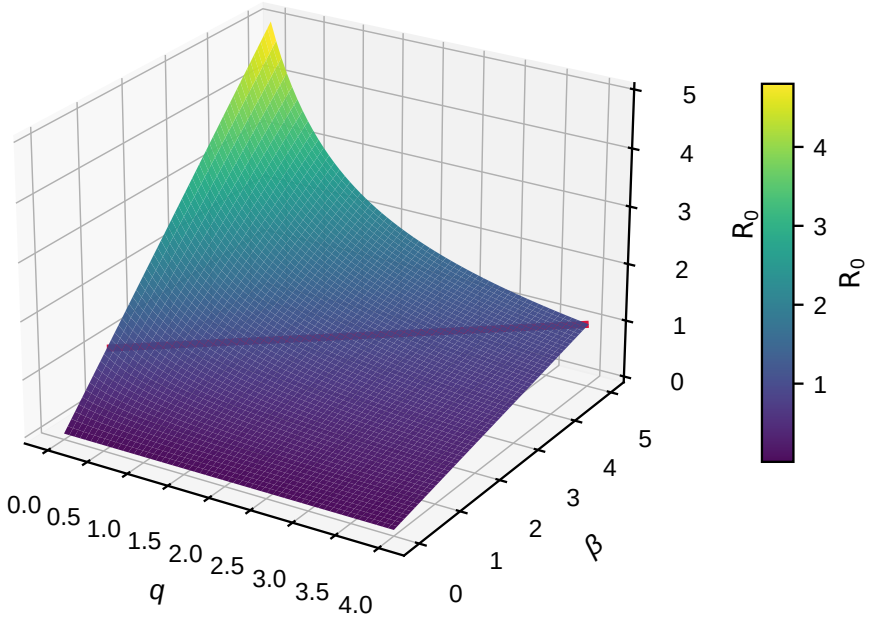

Fig. 3 The reproduction surface $\mathcal{R}_0 = \beta/(1+q)$ over the reduced parameter plane. The heavy contour marks the critical level $\mathcal{R}_0 = 1$

6.2 Transcritical bifurcation at the threshold

Anyway, through the two equilibrium branches (34)–(35) exchange stability at $\mathcal{R}_0 = 1$. Figure 7 traces the susceptible and infected components of both branches as $\mathcal{R}_0$ varies through unity: the disease-free branch $(s, i) = (1, 0)$ is stable for $\mathcal{R}_0 < 1$ and loses stability at $\mathcal{R}_0 = 1$, where the endemic branch $s^* = 1/\mathcal{R}_0$, $i^* = (1 - \mathcal{R}_0^{-1})/(1+q)$ emerges into the positive octant and takes over as the stable state. This is the standard forward (transcritical) bifurcation of a compartmental epidemic, made explicit here in the reduced coordinates.

6.3 Sensitivity of the threshold

However, because the threshold controls the qualitative outcome, its normalized forward sensitivity to each parameter is informative. For a quantity $\mathcal{R}_0$ depending on a parameter p, the normalized sensitivity index is $\Upsilon_p^{\mathcal{R}_0} = (\partial \mathcal{R}_0/\partial p)(p/\mathcal{R}_0)$. From (8) and (33),

$$\Upsilon_\Sigma^{\mathcal{R}_0} = \Upsilon_\gamma^{\mathcal{R}_0} = +1, \qquad \Upsilon_\alpha^{\mathcal{R}_0} = -\frac{2\alpha+\omega}{\alpha+\omega}, \qquad \Upsilon_\omega^{\mathcal{R}_0} = -\frac{\omega}{\alpha+\omega},$$
$$\Upsilon_\beta^{\mathcal{R}_0} = +1, \qquad \Upsilon_q^{\mathcal{R}_0} = -\frac{q}{1+q}. \tag{38}$$

Table 5 evaluates these at $\alpha = 0.5$, $\omega = 0.3$ (so $q = 0.6$), and Figure 8 displays them. Transmission enters with unit elasticity: a 1% rise in γ (or β) raises $\mathcal{R}_0$ by 1%. Natural mortality is the strongest

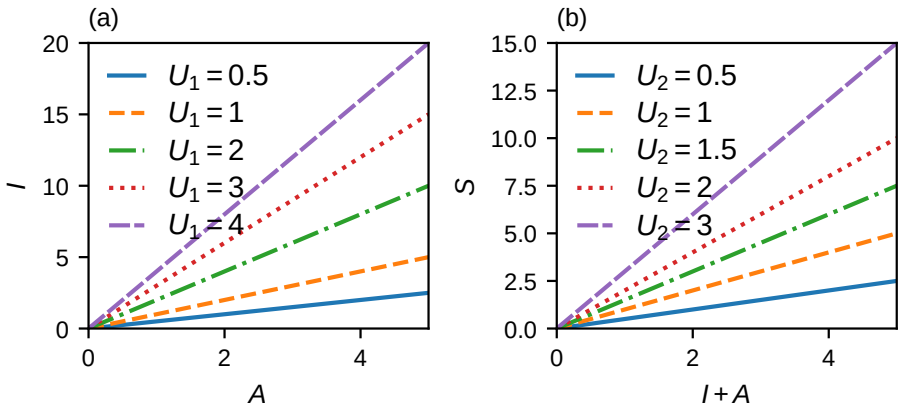

Fig. 4 The Invariant leaves of the scaling invariants. Each ray is a level set of (a) $U_1 = I/A$ in the (A, I) plane or (b) $U_2 = S/(I + A)$ in the $(I+A, S)$ plane, and is mapped into itself by the population dilation X_2

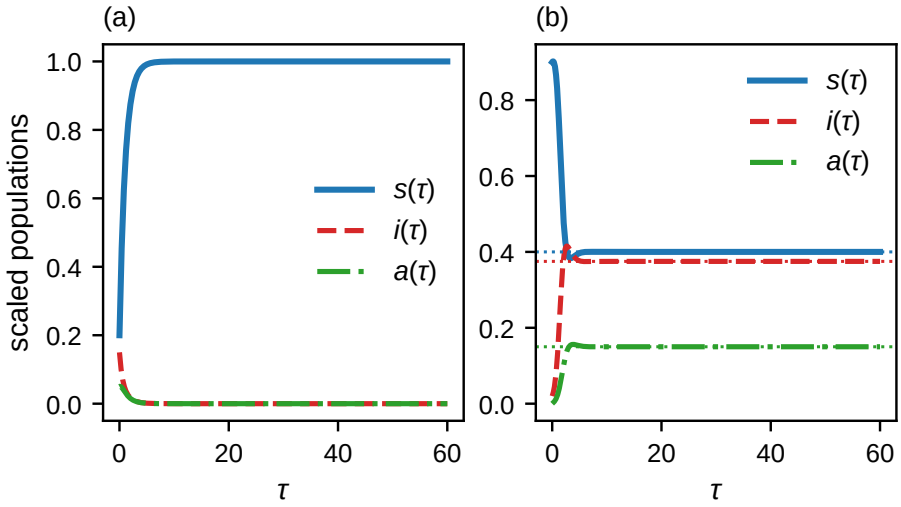

Fig. 5 Numerical solutions of the reduced system (30)–(32). (a) Disease-free regime $\mathcal{R}_0 = 0.5$: all infection decays and $s \to 1$. (b) Endemic regime $\mathcal{R}_0 = 2.5$: the solution converges to the endemic equilibrium (35) (dotted lines)

damping influence because it appears twice in (8), once in the demographic scale and once in the infectious period; progression ω (equivalently q) lowers $\mathcal{R}_0$ by shortening the infectious window before AIDS. The signs and magnitudes are exact analytic consequences of (8), not fitted quantities.

6.4 Structural summary

Figure 9 collects the exact structural counts of the analysis: three state variables, five dimensional parameters, a single fixed-parameter point symmetry, three equivalence generators, seven entries in the invariant map Π, and three reduced dimensionless parameters. The chart summarizes, at a glance, how far continuous symmetry reduces this model.

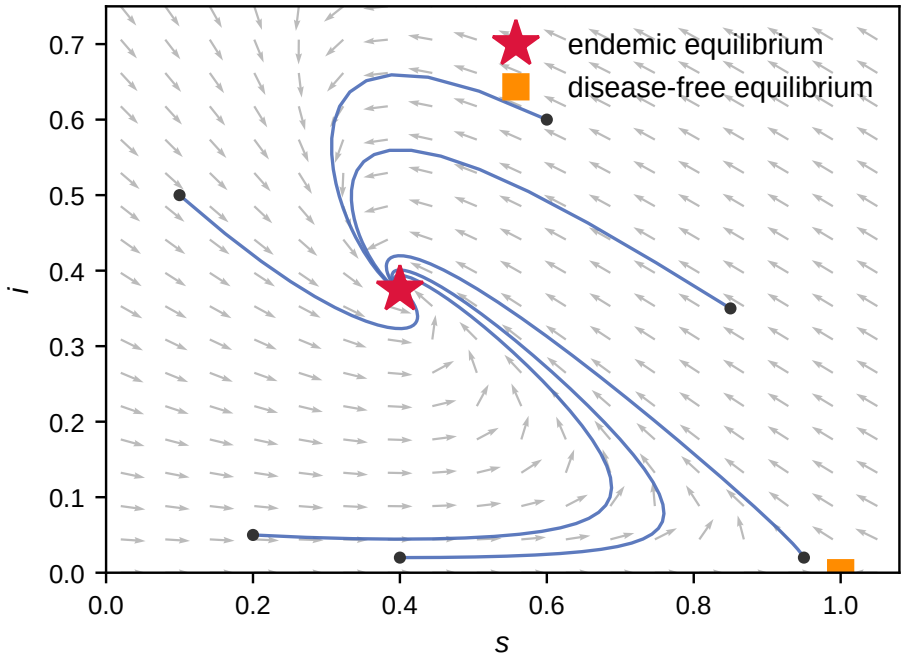

Fig. 6 The Phase portrait of the reduced model in the (s, i) plane for $\mathcal{R}_0 = 2.5$. Trajectories from several initial conditions converge to the endemic equilibrium (star); the disease-free equilibrium (square) is unstable. Arrows show the direction field

Table 5 Normalized forward sensitivity indices of $\mathcal{R}_0$, evaluated at $\alpha = 0.5$, $\omega = 0.3$ ($q = 0.6$). Positive indices raise the threshold; negative indices lower it.

Parameter	Σ	γ	α	ω	β	q
$\Upsilon_p^{\mathcal{R}_0}$	$+1.000$	$+1.000$	-1.625	-0.375	$+1.000$	-0.375

7 Nonautonomous coefficients and symmetry breaking

Interventions make the coefficients depend on time. Replacing the constant parameters by smooth functions gives

$$\dot{S} = \Sigma(t) - \gamma(t)SI - \alpha(t)S, \tag{39}$$

$$\dot{I} = \gamma(t)SI - \big[\alpha(t) + \omega(t)\big]I, \tag{40}$$

$$\dot{A} = \omega(t)I - \big[\alpha(t) + \delta(t)\big]A. \tag{41}$$

For $Q = \partial_t$ the determining equations (15) now retain the explicit t-derivatives of the coefficients, and the generator is admitted only when

$$\Sigma'(t) = \gamma'(t) = \alpha'(t) = \omega'(t) = \delta'(t) = 0. \tag{42}$$

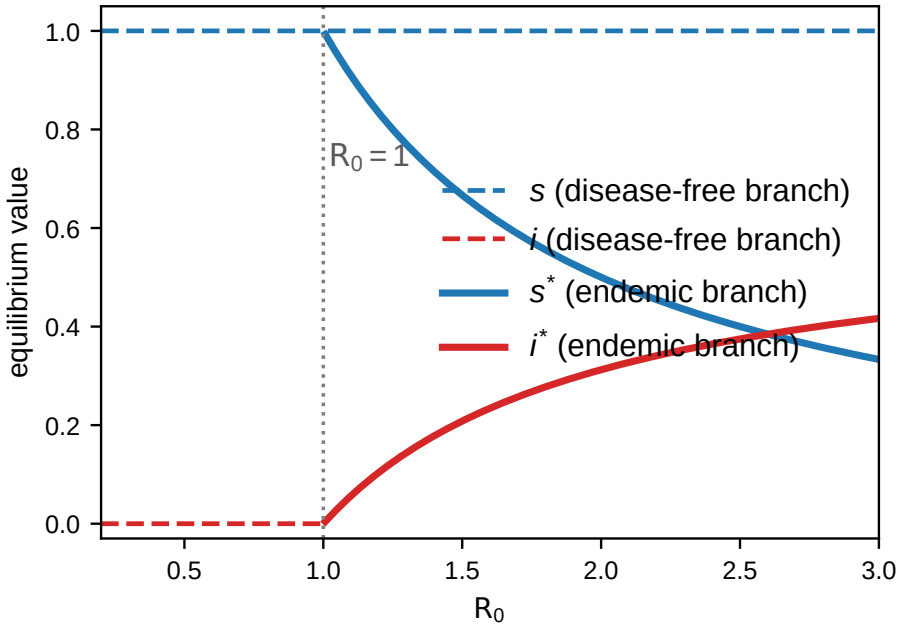

Fig. 7 Transcritical bifurcation of the reduced model at $\mathcal{R}_0 = 1$. The disease-free branch (dashed) is stable for $\mathcal{R}_0 < 1$; the endemic branch (solid) bifurcates into the positive octant at $\mathcal{R}_0 = 1$ and is stable for $\mathcal{R}_0 > 1$. Curves are drawn for $q = 0.6$

Any genuinely time-dependent intervention which means seasonal forcing, treatment scale-up, time-varying prevention, or behavioural change and proves therefore breaks the continuous time-translation symmetry X_0. The equivalence structure is more robust: transformations of the form (21) can still be formulated for the nonautonomous family, provided the coefficient *functions* transform consistently with (22), so the reduction of Section 5 survives in a parameter-function form even when the point symmetry does not.

8 Discussion

Looking at it closely, the corrected symmetry classification carries two lessons. First, autonomy guarantees the time-translation symmetry X_0, but a dissipative epidemic system of this kind carries no independent conserved quantity, so X_0 does not generate one; the search for a nonconstant first integral is not resolved by symmetry alone (Remark 1). Second, scaling the populations while freezing Σ and γ changes the equations, as the non-vanishing residuals (19)–(20) show. However, since such a scaling relates different members of the model family rather than different solutions of one fixed model. Keeping this straight prevents the orbit invariants of an equivalence group from being mistaken for constants along epidemiological trajectories which follows that a subtle error that the numerical experiment of Section 4.3 makes concrete by displaying two genuinely different models collapsing onto one reduced orbit.

So now, the reduced model (30)–(32) is valuable precisely because it isolates three interpretable

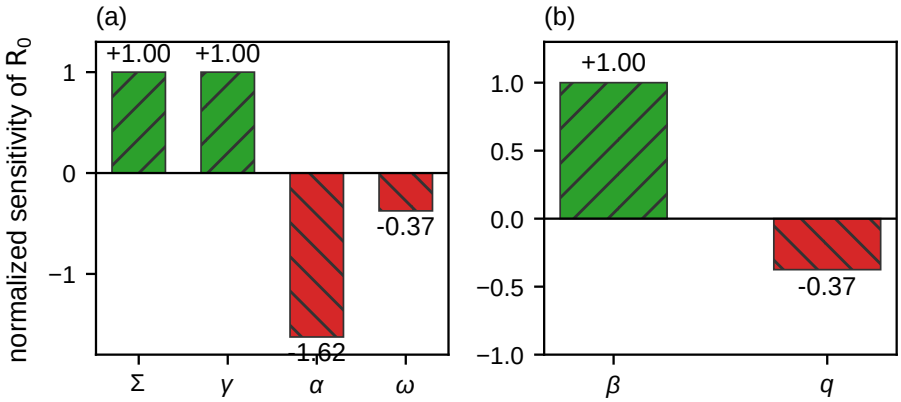

Fig. 8 Normalized forward sensitivity indices of $\mathcal{R}_0$ from (38), evaluated at $\alpha = 0.5$, $\omega = 0.3$. (a) Dimensional parameters; (b) reduced parameters. Upward, forward-hatched bars raise the threshold; downward, back-hatched bars lower it

combinations. The parameter β measures transmission on the natural demographic time scale, q measures progression relative to natural mortality, and d measures excess AIDS mortality on the same scale which we can't ignore. The threshold $\mathcal{R}_0 = \beta/(1+q)$ reproduces the next-generation result in dimensional variables, and the sensitivity indices (38) quantify how each mechanism moves it. This is the payoff of a symmetry reduction done correctly: a smaller, interpretable model with an exact map back to the original.

Indeed, the baseline model has clear limitations, and they bound the scope of the conclusions. It assumes homogeneous mixing, omits treatment and viral suppression, ignores vertical transmission and behavioural heterogeneity, treats the AIDS class as noninfectious, and is not calibrated to data. Its role is structural rather than predictive. Richer HIV models in the current literature add exactly the mechanisms it omits which brings to the fact that fractional memory (Silva and Torres 2019; Naik et al 2020a;b; Khan et al 2025), age structure and optimal control (Teklu et al 2025), drug resistance and vertical transmission (Peter et al 2025), PrEP (Silva and Torres 2018), stochastic forcing (Djordjevic et al 2018), with national calibration (Abidemi et al 2025; Xue et al 2023; Su et al 2026). These extensions enlarge the state and parameter spaces, but the equivalence methodology applies before any calibration or control step: it identifies redundant scales and the minimal set of dimensionless parameter combinations, shrinking the space that must be explored accurately. For spatial and age-structured models the recent Lie analyses of Naz, Torrisi, and Imran and of Cherniha and Davydovych show that admitted symmetries can go further and support exact reductions and closed-form solutions (Naz et al 2025; Naz and Torrisi 2024; Cherniha and Davydovych 2025; Cherniha et al 2024; Cherniha and Davydovych 2022), which suggests a natural continuation of the present work to structured HIV models.

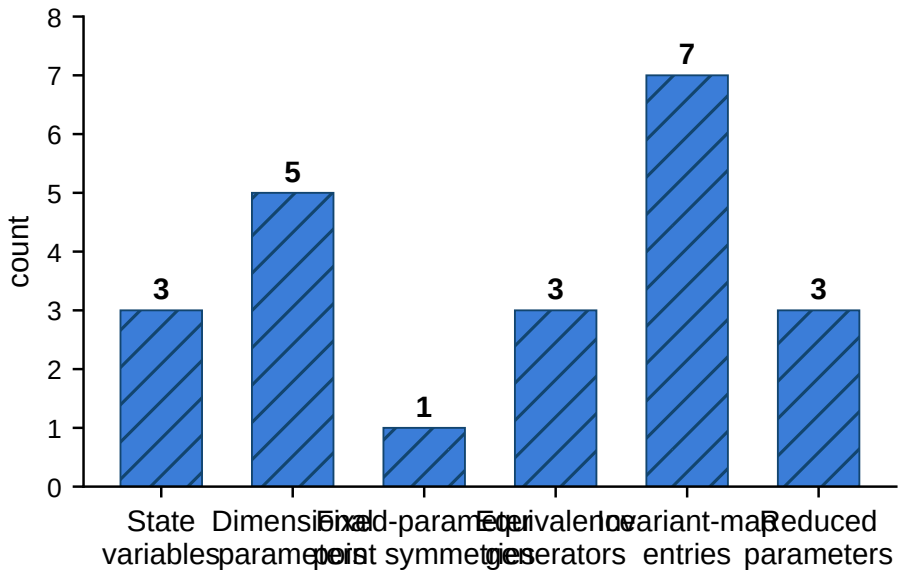

Fig. 9 The Exact structural counts of the analysis: three state variables, five dimensional parameters, one fixed-parameter point symmetry, three equivalence generators, seven invariant-map entries, and three reduced parameters

9 Conclusion and outlook

A direct Lie analysis of the susceptible–infected–AIDS model shows that time translation is the only elementary point symmetry for fixed parameters, while the intuitive population scalings are not symmetries at all: their prolonged residuals do not vanish. The scalings are recovered as equivalence transformations once recruitment and transmission parameters are rescaled with the populations, and together with time dilation they form a solvable three-parameter equivalence group. The joint invariants of the two commuting dilations reduce five parameters to three and return a compact dimensionless model whose flow reproduces the threshold, the endemic equilibrium, and the transcritical bifurcation of the full system. A numerical experiment confirms the equivalence group to eleven digits, and the sensitivity indices of the threshold follow in closed form.

We can see that the value of the result is methodological. It separates solution symmetries from model-family equivalences cleanly, it supplies a reduction with an exact inverse map, and it states precisely where time-dependent interventions destroy the continuous symmetry. These properties make it a reliable baseline for extending symmetry methods to treatment, behavioural, stochastic, fractional, age-structured, and spatial HIV models, where the same discipline which has proved that test the determining equations, never assume a first integral, and keep point symmetries apart from equivalences which implies that should carry over unchanged.

Statements and Declarations

Competing Interests The authors have no competing interests to declare that are relevant to the content of this article.

Funding This research received no specific grant from any funding agency in the public, commercial, or not-for-profit sectors.

Data availability No external datasets were generated or analysed during this study. Every figure and every numerical value reported in this article was computed directly from the model equations (1)–(3), the reduced system (30)–(32), the equilibrium relations (35), the equivalence relations (22), and the sensitivity formulae (38), using the parameter sets listed in Tables 4 and 5. The Python script that generates Figs. 1–9 from these equations is available from the corresponding author on request.

Author contributions S. O. Essang: conceptualization, methodology, formal analysis, software, writing – original draft. B. I. N.-I. Iserom: methodology, validation, writing – review and editing. T. A. Anake: formal analysis, validation, writing – review and editing. All authors read and approved the final manuscript.

Use of AI tools In preparing this manuscript the authors used a large language model (Claude, Anthropic) as an assistive tool for typesetting, for writing the Python code that computes Figs. 1–9 from the model equations, for locating and checking bibliographic records, and for language editing. The mathematical formulation, the symmetry and equivalence computations, and the interpretation of the results are the authors' own, and the authors have verified all analytical statements and numerical values reported here. The authors accept full responsibility for the content of this article.

References

Abidemi A, Fatmawati, Alfiniyah C, Windarto, Nyabadza F, Aziz MHN (2025) Insights into HIV/AIDS transmission dynamics and control in Indonesia: a mathematical modelling study. Partial Differ Equ Appl Math 14:101185. https://doi.org/10.1016/j.padiff.2025.101185

Attaullah, Zeb K, Khan I, Ahmad R, Eldin SM (2023) Transmission dynamics of a novel HIV/AIDS model through a higher-order Galerkin time discretization scheme. Sci Rep 13:7421. https://doi.org/10.1038/s41598-023-34696-6

Bluman GW, Cheviakov AF, Anco SC (2010) Applications of symmetry methods to partial differential equations. Applied Mathematical Sciences, vol 168. Springer, New York

Cherniha RM, Davydovych VV (2022) A reaction–diffusion system with cross-diffusion: Lie symmetry, exact solutions and their applications in the pandemic modelling. Eur J Appl Math 33:785–802. https://doi.org/10.1017/S0956792521000280

Cherniha R, Davydovych V (2025) An age-structured diffusive model for epidemic modelling: Lie symmetries and exact solutions. Qual Theory Dyn Syst 24:181. https://doi.org/10.1007/s12346-025-01340-9

Cherniha R, Dutka V, Davydovych V (2024) A space distributed model and its application for modeling the COVID-19 pandemic in Ukraine. Symmetry 16:1411. https://doi.org/10.3390/sym16111411

Diekmann O, Heesterbeek JAP, Metz JAJ (1990) On the definition and the computation of the basic reproduction ratio R_0 in models for infectious diseases in heterogeneous populations. J Math Biol 28:365–382. https://doi.org/10.1007/BF00178324

Djordjevic J, Silva CJ, Torres DFM (2018) A stochastic SICA epidemic model for HIV transmission. Appl Math Lett 84:168–175. https://doi.org/10.1016/j.aml.2018.05.005

Hydon PE (2000) Symmetry methods for differential equations: a beginner's guide. Cambridge University Press, Cambridge

Ibragimov NH (ed) (1994) CRC handbook of Lie group analysis of differential equations, vol 1: symmetries, exact solutions and conservation laws. CRC Press, Boca Raton

Khan M, Khan N, Ullah I, Shah K, Abdeljawad T, Abdalla B (2025) A novel fractal fractional mathematical model for HIV/AIDS transmission stability and sensitivity with numerical analysis. Sci Rep 15:9291. https://doi.org/10.1038/s41598-025-93436-0

Naik PA, Owolabi KM, Yavuz M, Zu J (2020a) Chaotic dynamics of a fractional order HIV-1 model involving AIDS-related cancer cells. Chaos Solitons Fractals 140:110272. https://doi.org/10.1016/j.chaos.2020.110272

Naik PA, Zu J, Owolabi KM (2020b) Modeling the mechanics of viral kinetics under immune control during primary infection of HIV-1 with treatment in fractional order. Physica A 545:123816. https://doi.org/10.1016/j.physa.2019.123816

Naz R, Torrisi M (2024) The closed-form solutions of an SIS epidemic reaction–diffusion model with advection in a one-dimensional space domain. Symmetry 16:948. https://doi.org/10.3390/sym16080948

Naz R, Torrisi M, Imran A (2025) Lie symmetries and solutions for a reaction–diffusion–advection SIS model with demographic effects. Symmetry 17:3. https://doi.org/10.3390/sym17010003

Olver PJ (1993) Applications of Lie groups to differential equations, 2nd edn. Graduate Texts in Mathematics, vol 107. Springer, New York

Peter OJ, Teklu SW, Balogun GB, Bolarin G, Asfaw MD (2025) HIV/AIDS compartmental model analysis with drug resistance treatment, vertical transmission, and optimal control theory. Sci Rep 15:44156. https://doi.org/10.1038/s41598-025-26943-9

Silva CJ, Torres DFM (2017) A SICA compartmental model in epidemiology with application to HIV/AIDS in Cape Verde. Ecol Complex 30:70–75. https://doi.org/10.1016/j.ecocom.2016.12.001

Silva CJ, Torres DFM (2018) Modeling and optimal control of HIV/AIDS prevention through PrEP. Discrete Contin Dyn Syst Ser S 11:119–141. https://doi.org/10.3934/dcdss.2018008

Silva CJ, Torres DFM (2019) Stability of a fractional HIV/AIDS model. Math Comput Simul 164:180–190. https://doi.org/10.1016/j.matcom.2019.03.016

Silva CJ, Torres DFM (2020) On SICA models for HIV transmission. In: Mathematical modelling and analysis of infectious diseases. Studies in Systems, Decision and Control, vol 302. Springer, Cham, pp 155–179. https://doi.org/10.1007/978-3-030-49896-2_6

Su L, Li W, Ma Y (2026) Modelling and analyzing the transmission dynamics of HIV/AIDS epidemic in China. J Biol Dyn 20:2622439. https://doi.org/10.1080/17513758.2026.2622439

Teklu SW, Guya TT, Kotola BS, Lachamo TS (2025) Analyses of an age structure HIV/AIDS compartmental model with optimal control theory. Sci Rep 15:5491. https://doi.org/10.1038/s41598-024-82467-8

van den Driessche P, Watmough J (2002) Reproduction numbers and sub-threshold endemic equilibria for compartmental models of disease transmission. Math Biosci 180:29–48. https://doi.org/10.1016/S0025-5564(02)00108-6

Xue L, Sun Y, Ren X, Sun W (2023) Modelling the transmission dynamics and optimal control strategies for HIV infection in China. J Biol Dyn 17:2174275. https://doi.org/10.1080/17513758.2023.2174275